JCTC Journal of Chemical Theory and Computation

Nonenzymatic Pathway of PUFA Oxidation. A First-Principles Study of the Reactions of OH Radical with 1,4-Pentadiene and Arachidonic Acid

Milan Szori,[‡,‡] Imre G. Csizmadia,[‡,§] and Bela Viskolcz*[,‡]

Department of Chemical Informatics, Faculty of Education, University of Szeged, Boldogasszony sgt. 6, 6725 Szeged, Hungary, Institute of Organic Chemistry and Biochemistry, Academy of Sciences of the Czech Republic, Flemingovo náměstí 2, 16610 Prague 6, Czech Republic, and Department of Chemistry, University of Toronto, Toronto, Ontario, Canada M5S 3H6

Received April 14, 2008

Abstract: The oxidation of polyunsaturated hydrocarbons by ·OH radical can play an important role in lipid oxidation of polyunsaturated fatty acids (PUFA) such as arachidonic acid (AA). As a prototype of this oxidation, the reaction of 1,4-pentadiene with the ·OH radical is studied using the QCISD(T)/cc-pVTZ//BH&HLYP/6−31G(d) level of theory. One of the prereaction complexes is shown to be a springboard for the indirect bisallylic hydrogen abstraction (A_O), terminal ($T0_O$), and nonterminal ·OH addition ($NT0_O$) reactions. The enthalpies of the transition states of the A_O, $T0_O$, and $NT0_O$ reactions are found to be lower than those of the reactants, so all these reactions are expected to be fast. The nonterminal adduct is found to be reactive *via* two low-lying consecutive reaction channels. The first channel is a five-membered ring closing ($NT1_O$). The second channel is bond scission, which results in an allyl radical and a vinyl alcohol ($NT2_O$). An analogous reaction pathway in which AA takes the place of 1,4-pentadiene was explored using the ONIOM(QCISD(T)/cc-pVTZ:BH&HLYP/6−31G(d))//BH&HLYP/6−31G(d) method. The results show that the formation of the five-membered ring (AA-$NT1_O$) is energetically favored. Our results demonstrate for the first time a possible, *ab initio*-based mechanism for the nonenzymatic biosynthesis of isoprostane-like structures from AA without the presence of molecular oxygen. Furthermore, the energetically low-lying bond scission channel may explain the observed formation of short fatty acids and dieneols (tautomers of unsaturated aldehydes).

1. Introduction

Fatty acids (FAs) are essential components of membrane phospholipids. The hydrocarbon chain of the FAs can be saturated as well as either monounsaturated (MUFA) or polyunsaturated (PUFA). An important subclass of PUFAs, called $\omega-6$ fatty acids, can be characterized by a double bond network which starts from the sixth carbon−carbon bond counting from the methyl carbon at the tail end (ω end) of the fatty acid.

PUFAs are integral structural components of membrane phospholipids, where they play an important role in maintaining the structural and functional characteristics of bilayer cell membranes within their homeostatic boundaries. Besides their physical effects on the membrane, PUFAs also contribute to regulatory function through eicosanoid production.[1] Eicosanoids are physiologically active compounds derived biosynthetically from 20-carbon fatty acids following their release from the membrane, through the specific action of phospholipase A2, and include prostaglandins, thromboxanes, and leukotrienes.[2]

Arachidonic acid (AA, 20:4n-6) is an $\omega-6$ fatty acid which is highly concentrated in brain tissue as an essential

* Corresponding author e-mail: viskolcz@jgypk.u-szeged.hu.
‡ University of Szeged.
‡ Academy of Sciences of the Czech Republic.
§ University of Toronto.

10.1021/ct800127a CCC: $40.75
Published on Web 08/02/2008

Scheme 1. Structure of Arachidonic Acid and 1,4-Pentadiene[a]

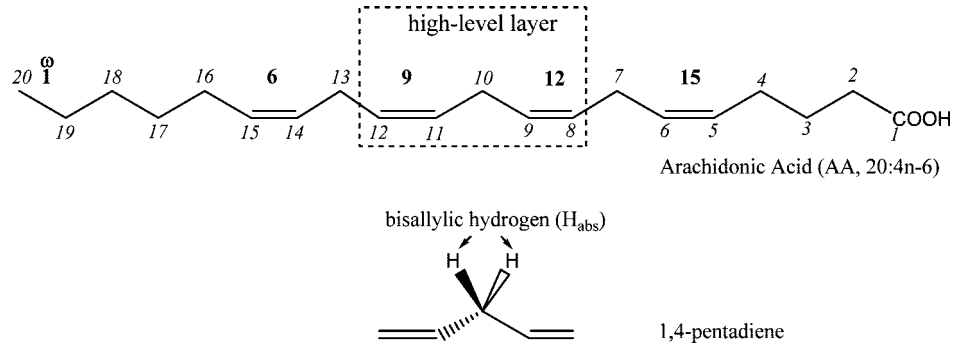

[a] The box with dotted lines shows the definition of the high-level layer in the ONIOM calculation.

component of membrane phospholipids.[3] Arachidonic acid is the most important prostaglandin precursor in humans,[4] and it is a component of the inositol phospholipids. AA plays a role in eicosanoid synthesis, such as the biosynthesis of 15-F_2-isoprostane. The conventional view of isoprostane synthesis proceeds *via* a pathway,[5] which begins with the formation of a radical by abstraction of the bisallylic hydrogen (H_{abs}) on C13 of AA (Scheme 1). Then, after several reaction steps, a five-membered ring is formed from C8−C12 carbons by means of molecular oxygen, producing isoprostanes.

There are several shortcomings to this view. The formation of isoprostanes has been detected in the nonenzymatic oxidation of the membrane *in vivo* and *in vitro*.[6,7] Furthermore, the conventional view cannot account for observation of unsaturated aldehydes in the oxidation of the membrane compounds.[8] However, mechanistic steps for the nonenzymatic pathway have not been established theoretically.

Our aim in this work is to gain a better understanding of the nonenzymatic pathway. From a reactivity point of view, 1,4-pentadiene (Scheme 1) is a good candidate for elucidating possible oxidation pathways of PUFAs. The reaction 1,4-pentadiene + ·OH has other advantages, such as the moderate computational effort needed to perform the calculation and the absence of steric effects.

This paper is organized as follows. Section 2 describes the quantum chemical methods used for geometry optimizations and high-level energy calculation. Section 3 describes the prereaction complexes and the associated low-lying channels for the 1,4-pentadiene + ·OH reaction, including transition states and products. Having established possible pathways for 1,4-pentadiene, similar calculations are carried out for arachidonic acid (AA) in place of 1,4-pentadiene.

2. Methods

All calculations were performed by using the Gaussian03 program package.[9] In the case of reactions between alkenes and the hydroxyl radical, it has been shown previously[10] that the BH&HLYP functional gives reasonable geometries when used in combination with the 6−31G(d) split-valence basis set.[11] In every geometry optimization, 'Tight' convergence criteria were used. The nature of stationary points was checked by means of frequency calculations. Analytical second derivatives of the energy with respect to Cartesian coordinates were used for the determination of vibrational frequencies. Furthermore, additional and accurate single point calculations were carried out on the BH&HLYP/6−31G(d) geometries using the QCISD(T) method[12,13] along with the cc-pVTZ Dunning basis set.[14] Intrinsic reaction coordinate (IRC) calculation started from the A_O transition state was also computed using the BH&HLYP/6−31G(d) level of theory.

The structures in reactions of AA + ·OH were also optimized at the BH&HLYP/6−31G(d) level of theory. Accurate single point energies were computed using the two-layer ONIOM technique,[15] employing the QCISD(T)/cc-pVTZ and the BH&HLYP/6−31G(d) level of theories for the high-level and low-level layers, respectively. The high-level layer contains C8−C12 and connected hydrogens, as illustrated in Scheme 1. These calculations are referred to as ONIOM(QCISD(T)/cc-pVTZ:BH&HLYP/6−31G(d))// BH&HLYP/6−31G(d).

Activation enthalpies ($\Delta^{\ddagger}H°$) are calculated as the difference of QCISD(T)/cc-pVTZ energies between the transition state (TS) structure and the van der Waals complex (COM), adding the difference of their corresponding enthalpies calculated at the BH&HLYP/6−31G(d) level of theory, and without any scale correction (Scheme 2). The electronic partition function of a species is assumed to be equal to its multiplicity. In the case of the consecutive steps ($NT1_O$ and $NT2_O$ as well as AA-$NT1_O$ and AA-$NT2_O$), the nonterminal adduct is regarded as the reactant, rather than the prereaction complex (COM). The relative enthalpies of the transition state ($\Delta H°_{rel}$(TS)) are related to the enthalpy level of the reactants (1,4-pentadiene and hydroxyl radical). The same nomenclature is used in the case of the AA + ·OH reaction; the only difference is the ONIOM(QCISD(T)/cc-pVTZ: BH&HLYP/6−31G(d)) energy term instead of QCISD(T)/cc-pVTZ.

In the case of AA + ·OH reactions, the effects of the surrounding lipid are also estimated though BH&HLYP/6−31G(d) single-point calculation using the CPCM model.[16] The solute cavity is built up by means of radii from the UFF force field (RADII = UFF). A value of 4.0 was employed for the dielectric constant (ϵ), to simulate the hydrophobic interior of a lipid membrane. All the remaining parameters

Scheme 2. Schematic Picture about the Definition of Different Thermodynamic Properties[a]

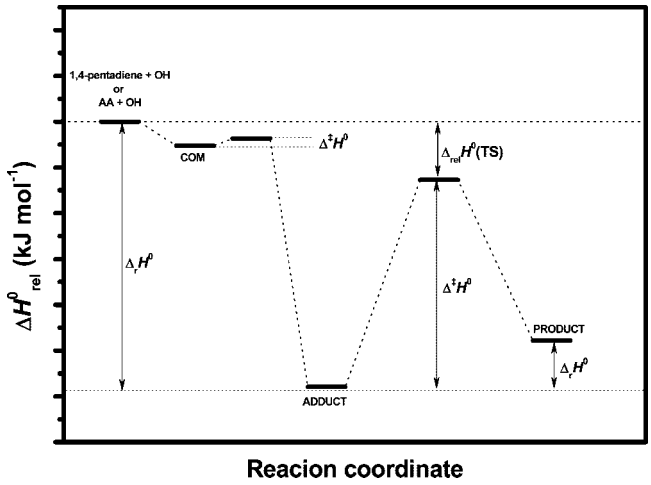

[a] Enthalpy, *H*, is the example, and it is also valid for entropy and Gibbs free energy.

for the surrounding lipid are the same as those for water. The contribution of the solvation to activation and reaction Gibbs free energies, $\Delta\Delta G^{\circ}_{solv}(X)$, are formulated as

$$\Delta\Delta G^{\circ}_{solv}(X) = \Delta G^{\circ}_{solv}(X) - \Delta G^{\circ}_{solv}(AA + {}^{\bullet}OH)$$

3. Results and Discussion

Reactions of 1,4-Pentadiene and Hydroxyl Radical. It is well-known that in alkene + ·OH reactions,[10,17,18] the first step is the formation of a prereaction complex (COM). Depending on the orientation of the ·OH radical, one can distinguish two possible van der Waals complexes (COM_O and COM_I in Figure 1). In the outer complex (COM_O), the ·OH radical is further from the center of the mass of the complex. For the inner one (COM_I), the ·OH radical is closer to the center of mass of the van der Waals complex. Despite this structural difference, both complexes exhibit rather similar standard reaction enthalpies (Table 1). The outer complex, COM_O, is the initial structure for the terminal (T_O) and nonterminal additions (NT_O) as well as for the indirect hydrogen abstraction (A_O) reactions. In contrast to this, the indirect hydrogen abstraction cannot take place in COM_I, since the distance between the closest hydrogen and the oxygen is too large (3.876 Å) as can be seen in Figure 1. The corresponding distance in COM_O is only 2.826 Å, but the two van der Waals complexes are almost identical in the rest of the geometrical parameters. In the IRC calculation started from transition state of A_O, the ·OH radical approaches the double bond of the 1,4-pentadiene which shows that there is a pathway between A_O and COM_O.

The difference between the standard reaction entropies for the complex formation is 6.3 J mol^{-1} K^{-1}, which might be due to the interaction of the oxygen with the bisallylic hydrogen (H_{abs}). This difference has only a small contribution to the standard reaction Gibbs free energy (Table 1). Our calculations show that there is no significant energetic difference between the existing reaction channels started from the COM_O and the COM_I (the maximum deviation is smaller

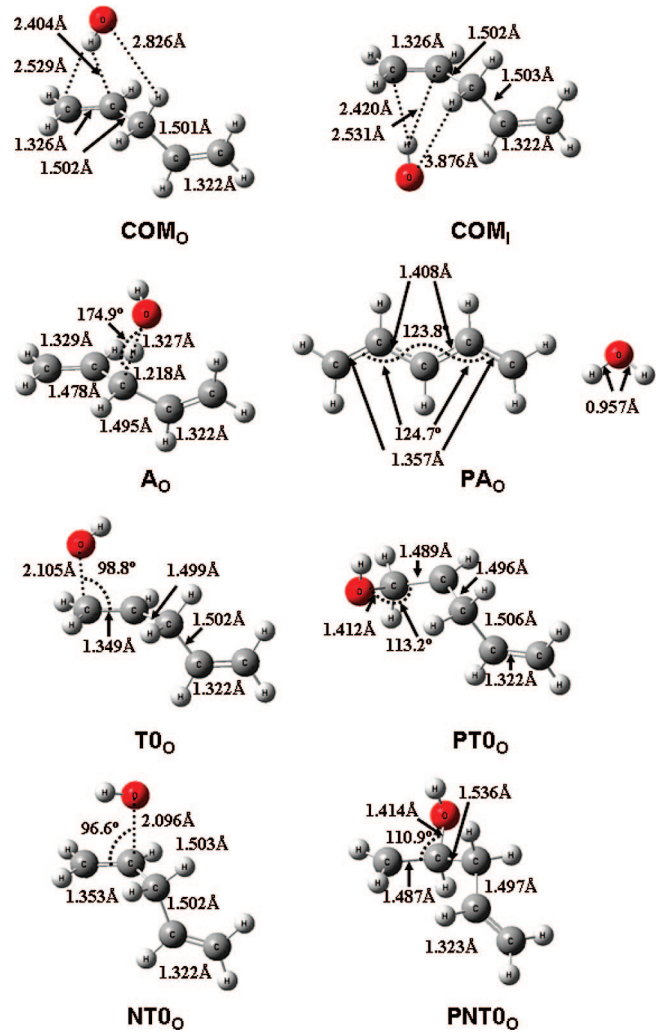

Figure 1. BH&HLYP/6−31G(d) optimized structures of the inner (COM_I) and outer (COM_O) prereaction complexes as well as minimum and transition state structures of the terminal addition ($T0_O$, $PT0_O$), indirect abstraction (A_O, PA_O), and nonterminal addition ($NT0_O$, $PNT0_O$) channels in the 1,4-pentadiene + ·OH reaction system.

than 2.5 kJ mol^{-1}). Thermodynamic properties of all these reactions are listed in Table 1. Because the addition reactions from COM_O and COM_I differ in chirality and structural parameters, so they differ slightly in enthalpy. Due to this, the order of channels in the activation enthalpy can be changed. These effects are rather small.

As Figure 2 shows, all of channels associated with COM_O have transition states that are below the entrance enthalpy level. The energetically most favored channel is the indirect hydrogen abstraction (A_O) reaction ($\Delta H^{\circ}_{rel} = -8.0$ kJ mol^{-1}, $\Delta^{\ddagger}H^{\circ} = 2.5$ kJ mol^{-1}). The products of this reaction are the resonance stabilized 1,4-pentadien-3-yl and a water molecule (PA_O). This reaction can also be considered as a prototype for bisallylic H-abstraction reactions, since the 1,4-pentadien-3-yl radical has five electrons delocalized on five carbon atoms,[19] which is a conjugated diallyl radical. The reaction is strongly exothermic (−167.9 kJ mol^{-1}). Its transition state structure (A_O) shows strongly reactant-like behavior, since the O−H_{abs} distance (1.327 Å) is significantly larger than the O−H distance (0.957 Å) in the water molecule. The

Table 1. Standard Reaction, Activation, and Relative Enthalpies ($\Delta_r H°$, $\Delta^{\ddagger}H°$, and $\Delta H°_{rel}$(TS) in kJ mol^{-1}) and Standard Reaction and Activation Entropies ($\Delta_r S°$ and $\Delta^{\ddagger}S°$ in J mol^{-1}K^{-1}) for the Reactions of 1,4-Pentadiene with the Hydroxyl Radical, Obtained from Calculations Performed at the QCISD(T)/cc-pVTZ//BH&HLYP/6-31G(d) Level of Theory

	$\Delta_r H°$ (kJ mol^{-1})	$\Delta_r S°$ (J mol^{-1} K^{-1})	$\Delta_r G°$ (kJ mol^{-1})	$\Delta H°_{rel}$(TS) (kJ mol^{-1})	$\Delta^{\ddagger}H°$ (kJ mol^{-1})	$\Delta^{\ddagger}S°$ (J mol^{-1} K^{-1})	$\Delta^{\ddagger}G°$ (kJ mol^{-1})
				Outer			
COM_O	−10.5	−99.7	19.2	-	-	-	-
A_O	−167.9	5.3	−169.5	−8.0	2.5	−22.8	9.3
$T0_O$	−110.4	−128.5	−72.1	−5.7	4.8	−22.7	11.6
$NT0_O$	−115.9	−136.1	−75.3	−7.3	3.2	−28.5	11.7
$NT1_O$	−78.4	−32.4	−68.7	−45.4	70.5	−32.6	80.2
$NT2_O$	20.3	157.3	−26.6	−25.5	90.4	0.4	90.3
				Inner			
COM_I	−11.8	−106.0	19.8	-	-	-	-
$T0_I$	−111.3	−131.3	−72.2	−9.2	2.6	−25.7	10.3
$NT0_I$	−118.2	−139.1	−76.8	−6.9	4.9	−26.2	12.7
$NT1_I$	−76.1	−29.5	−67.3	−47.9	70.3	−28.7	78.9
$NT2_I$	22.6	161.3	−25.4	−26.6	91.7	2.1	91.0

C−H_{abs} bond being broken (1.218 Å) is larger by 0.128 Å than that in 1,4-pentadiene (1.090 Å). Due to the exothermicity of this reaction, one may expect a low probability of occurrence for the reverse reaction, an expectation that is reinforced by the fact that the forward reaction has a large negative standard Gibbs free energy (−169.5 kJ mol^{-1}, Table 1).

The reaction with the highest activation enthalpy is the terminal addition ($T0_O$). If one compares the enthalpy of $T0_O$ to that of COM_O, then the enthalpy barrier is 4.8 kJ mol^{-1}. In this case, the product is a stable 4-pentenyl-1-ol radical ($PT0_O$). As one can see from Figure 1, the oxygen of the ·OH radical is still far (2.105 Å) from the terminal carbon in the transition state of the terminal addition ($T0_O$). In the case of the product, $PT0_O$, the C−O distance becomes shorter (1.412 Å), while the C═C bond extends to 1.489 Å, so it becomes more single bond like. The O−C−C angle increases from 98.8° to 113.2°.

The transition states for the possible consecutive reaction steps from the adducts $PT0_O$ and $PNT0_O$ were also characterized at the BH&HLYP/6−31G(d) level of theory (see the Supporting Information). In most cases, their relative enthalpies were found to be 20 kJ mol^{-1} higher than the entrance enthalpy. As it will be shown later on, these channels are energetically unfavored in contrast to the two corresponding channels of the nonterminal adduct. Due to this fact, contribution of these channels to the overall kinetics is expected to be negligible at room temperature, so they are not considered further.

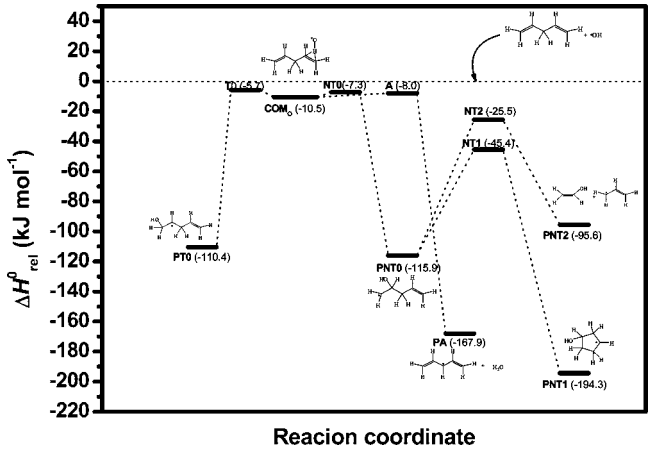

Figure 2. Standard enthalpy diagram for the energetically preferred reactions of 1,4-pentadiene with ·OH. The values are obtained at the QCISD(T)/cc-pVTZ//BH&HLYP/6−31G(d) level of theory.

The third reaction channel studied is the nonterminal addition reaction ($NT0_O$). Its enthalpy is 3.2 kJ mol^{-1} relative to that of COM_O (Table 1). The geometrical parameters of the nonterminal transition state are quite similar to that of the terminal one (Figure 1). In this case, the oxygen of the hydroxyl radical is also found to be far from the carbon, 2.096 Å. The C−C−O angle is also close to perpendicular, 96.6°.

Although the geometry of the 4-pentene-2-ol-1-yl radical formed ($PNT0_O$) also shows similarities to $PT0_O$, it is more reactive, since there are two possible low-lying transition states. The energetically preferred one is the ring closing reaction, $NT1_O$, which gives the cyclopentanol-3-yl radical, $PNT1_O$. Although the enthalpy barrier of this reaction seems to be rather large, 70.5 kJ mol^{-1}, it is still below the enthalpy level of the entrance channel, −45.4 kJ mol^{-1}. It is also interesting to note that the ring closing reaction is also exothermic ($\Delta_r H°(NT1_O) = -78.4$ kJ mol^{-1}). The enthalpy level of the cyclopentanol-3-yl radical is 26.4 kJ mol^{-1} lower than that of the product of the hydrogen abstraction, so the product radical is 194.3 kJ mol^{-1} more stable compared to the level of 1,4-pentadiene and hydroxyl radical. In its transition state (Figure 3), the distance between the two terminal carbons is 2.231 Å, which is about 0.7 Å larger than that found in the product (1.533 Å). The latter distance is in accord with a single carbon−carbon bond. The C−C···C and C···C−C angles also change significantly on going from the transition state to the product (Figure 3), the former extending from 87.8° to 104.2°, while the latter is 88.6° in the transition state structure and 103.4° in the product.

The other channel is the carbon−carbon bond scission, which gives vinyl alcohol as well as allyl radical as products ($PNT2_O$). Its transition state is product-like, as one can see from Figure 3. The broken bond distance is somewhat larger than 2.0 Å in the transition state, 2.096 Å. The enthalpy of

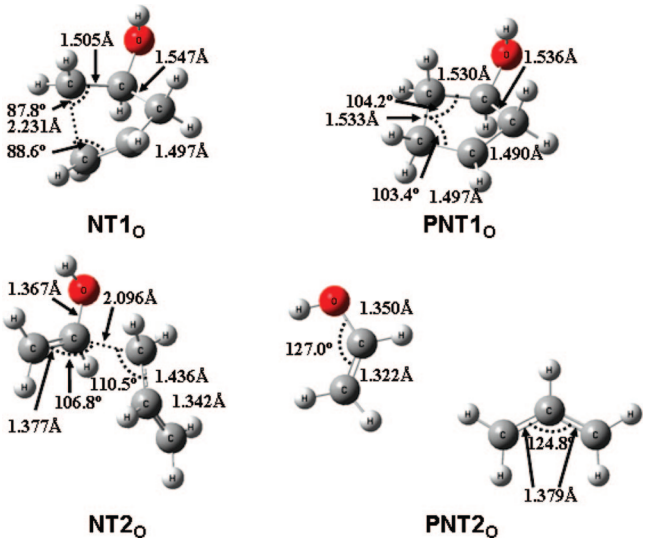

Figure 3. BH&HLYP/6−31G(d) optimized transition state structures for the five-membered ring formation reaction ($NT1_O$) and for the bond dissociation reaction ($NT2_O$) from the nonterminal addition adduct ($PNT0_O$).

$NT2_O$ is 90.4 kJ mol^{-1} relative to $PNT0_O$, and the reaction itself is slightly endothermic ($\Delta_r H°(NT2_O) = 22.6$ kJ mol^{-1}). Surprisingly, the standard activation entropy is close to zero (0.4 J mol^{-1} K^{-1}), and the reverse reaction has also a relatively large enthalpy barrier (70.1 kJ mol^{-1}). This value indicates that the bimolecular reverse reaction is not favored energetically. Thermodynamically, $PNT2_O$ is favored over $PNT0_O$ at room temperature.

Interestingly, 1,4-pentadiene is not only important as a model of PUFAs but also is found in mineral and vegetable oils. Consequently, its oxidation by hydroxyl radical also has a great impact on combustion chemistry.[20,21] Furthermore, the polyunsaturated hydrocarbons are also known to be present in the atmosphere as anthropogenic and biogenic volatile organic compounds (VOC).[22,23]

Reactions of Arachidonic Acid (AA) with Hydroxyl Radical. Given its relevance, the oxidation of arachidonic acid (AA) is frequently assayed using a wide variety of experimental setups, including HPLC/MS/MS.[6,7] Although these experiments are state-of-the-art, only stable products can be detected. Since abstraction of hydrogen by the ·OOH radical cannot be fast at the bisallylic position,[10] the ·OH radical is considered as a radical source in the first step of lipid peroxidation.[5] This prompted us to study possible initial steps for the AA oxidation by the ·OH radical.

For several $\omega-3$ PUFA species, different conformations were studied. The extended conformer was found to be the global minimum in vacuum.[24] Based on this result, the extended conformer of AA was used as an initial structure in our work. The reactions studied can be found in Figure 4, using the analogy of the 1,4-pentadiene + ·OH reaction involving hydrogen abstraction ($AA\text{-}A_O$) and nonterminal-like addition ($AA\text{-}NT0_O$) and its consecutive steps ($AA\text{-}NT1_O$ and $AA\text{-}NT2_O$). All of these channels were found, and the optimized structures of their corresponding critical points are shown in Figure 5. There are four double bonds in AA, and each may form a van der Waals complex (the ·OH radical

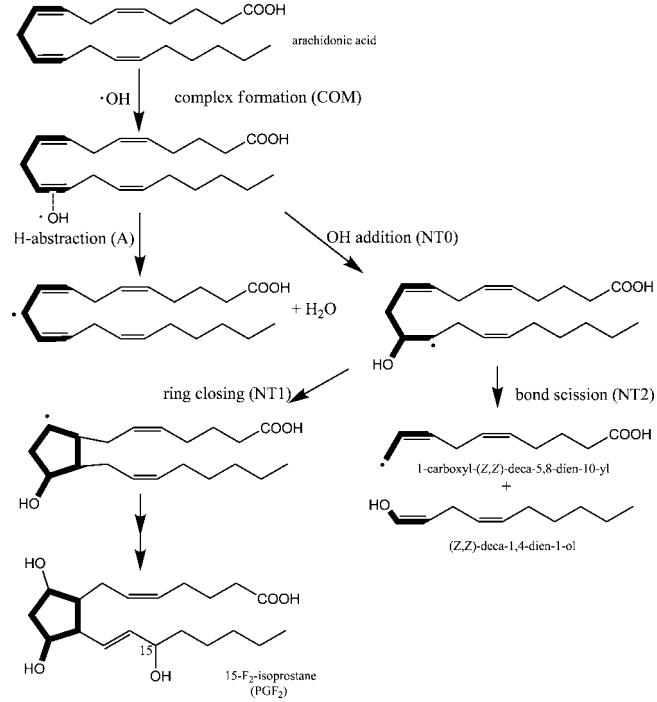

Figure 4. Possible nonenzymatic pathways for oxidation of arachidonic acid (AA) as a lipid-oxidation example. The pathways are suggested based on the radical reaction of 1,4-pentadiene with the hydroxyl radical. The pattern of 1,4-pentadiene is indicated by thick lines.

can approach the AA at the $\omega-6$, $\omega-9$, $\omega-12$, and $\omega-15$ positions, using the notation of Scheme 1). We only consider the AA + ·OH reactions *via* the $\omega-9$ van der Waals complex in this work (Figure 4), since our aim is to show the mechanism of formation of isoprostane-like species. There is no doubt that reactions involving other types of prereaction complexes ($\omega-6$ or $\omega-12$ or $\omega-15$) can also occur, since the bond energies of bisallylic hydrogens do not depend strongly on their position in the chain.[25] In these cases, only the positions of the five-membered rings in $AA\text{-}PNT1_O$ as well as the sizes of the carbon chains in the products of $AA\text{-}PNT2_O$ would vary.

Comparison of Figure 5 with Figure 1 and Figure 3 shows generally a good structural agreement between the 1,4-pentadiene and the AA reactions. Two exceptions stand out: the different is a little larger in comparisons of $AA\text{-}COM_O$ vs COM_O as well as $AA\text{-}A_O$ vs A_O, respectively. The ·OH and C═C double bond are somewhat closer in the $AA\text{-}COM_O$. This could be the consequence of the steric effects in the case of weakly bonded structures. The transition state of the abstraction reaction ($AA\text{-}A_O$ in Figure 5) seems to be of a more earlier type compared to that of 1,4-pentadiene and ·OH (A_O in Figure 1), since the $O\cdots H_{abs}$ is found to be 1.405 Å which is 1.327 Å in the case of the 1,4-pentadiene reaction. Furthermore, the $C\cdots H_{abs}$ distance also becomes shorter by 0.029 Å.

If one compares the values in Table 1 to those in Table 2, the difference in enthalpy between 1,4-pentadiene and corresponding AA reactions are in general less than 11 kJ mol^{-1}. The single exception is the reaction enthalpy of the ring closing reaction, $NT1_O$, 27.1 kJ mol^{-1}. This difference

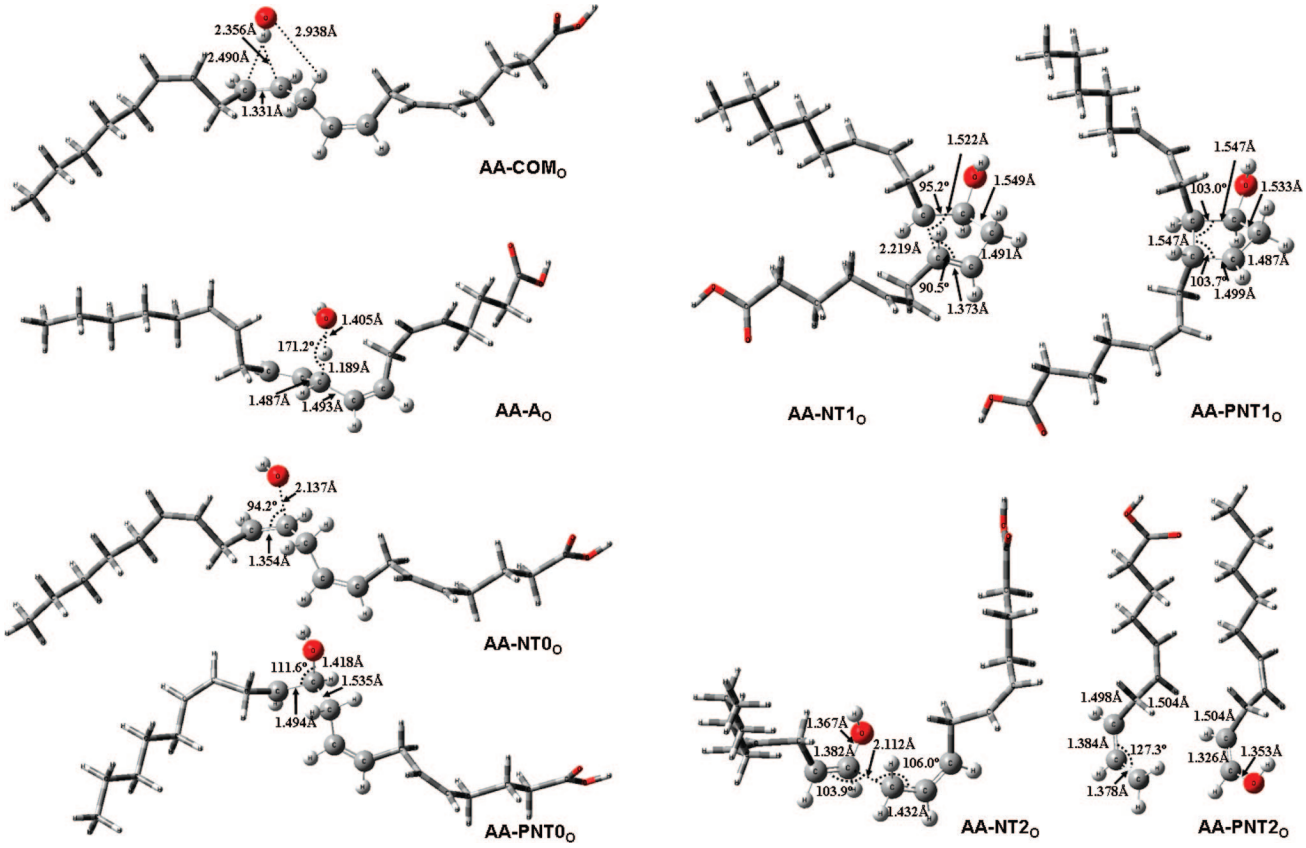

Figure 5. Transition state and minimum structures for the reactions of arachidonic acid (AA) with •OH radical, obtained at the BH&HLYP/6−31G(d) level of theory.

Table 2. Standard Reaction, Activation, and Relative Enthalpies ($\Delta_r H°$, $\Delta^‡ H°$, and $\Delta H°_{rel}$(TS) in kJ mol^{-1}) and Standard Reaction and Activation Entropies ($\Delta_r S°$ and $\Delta^‡ S°$ in J mol^{-1} K^{-1}) for the Reactions of Arachidonic Acid (AA) with the Hydroxyl Radical, Obtained from Calculations at the ONIOM(QCISD(T)/cc-pVTZ:BH&HLYP/6-31G(d))//BH&HLYP/6-31G(d) Level of Theory[a]

	$\Delta_r H°$ (kJ mol^{-1})	$\Delta_r S°$ (J mol^{-1} K^{-1})	$\Delta_r G°$ (kJ mol^{-1})	$\Delta H°_{rel}$(TS) (kJ mol^{-1})	$\Delta^‡ H^0$ (kJ mol^{-1})	$\Delta^‡ S^0$ (J mol^{-1} K^{-1})	$\Delta^‡ G^0$ (kJ mol^{-1})
			Outer				
AA-COM$_O$	−13.1	−115.8	21.4 (4.7)	-	-	-	-
AA-A$_O$	−173.6	7.5	−175.9 (−10.8)	−10.0	3.1	−36.4	13.9 (−3.4)
AA-NT0$_O$	−123.2	−146.8	−79.4 (0.3)	−12.4	0.7	−16.8	0.7 (−0.1)
AA-NT1$_O$	−51.3	−46.5	−37.4 (−6.3)	−56.0	67.2	−39.5	78.9 (10.8)
AA-NT2$_O$	26.1	169.8	−24.5 (−3.9)	−29.4	93.8	3.7	92.7 (0.8)

[a] Values in parentheses are the contributions of the bulk solvation (lipid) to Gibbs free energy ($\Delta\Delta G°_{solv}$) calculated by CPCM-BH&HLYP/6-31G(d) single point calculation ($\epsilon = 4.0$).

may be due to a steric constraint caused by the ring formed in the reaction.

Furthermore, the AA-A$_O$ and AA-NT0$_O$ activation enthalpies are slightly negative (−1.5 and −3.0 kJ mol^{-1}, respectively). Compared to the activation enthalpies of 1,4-pentadiene and AA reaction systems, the difference is found to be as small as 0.6 kJ mol^{-1} for A$_O$, −2.5 kJ mol^{-1} for NT0$_O$, −3.3 kJ mol^{-1} for NT1$_O$, and 3.4 kJ mol^{-1} for NT2$_O$.

The most important result to emphasize is that the transition states for the AA + •OH reaction system are ring closing and bond scission, and these states lie energetically below the entrance enthalpy level (AA + •OH). The product of the ring closing reaction is AA-PNT1$_O$. The bond scission reaction produces a shortened fatty acid, 1-carboxyl-(Z,Z)-deca-5,8-diene-10-yl radical, and an eneol, the (Z,Z)-deca-1,4-diene-1-ol molecule (Figure 4 and Figure 5). The (Z,Z)-deca-1,4-diene-1-ol might convert to its tautomer, Z-4-ene-decanal. However, subsequent reactions become far too complex to be characterized since the number of possible reactions increases with the number of components.

The effects of the surrounding lipids are estimated using the CPCM model (Table 2) for the reaction system AA + •OH. The largest contribution of solvation to reaction Gibbs free energy is found in the case of the hydrogen abstraction ($\Delta\Delta_r G°_{solv}$(AA-A$_O$) = −10.8 kJ mol^{-1}). All the remaining $\Delta\Delta_r G°_{solv}$ are moderate with absolute values less than 7 kJ mol^{-1}. The largest contribution of solvation to activation Gibbs free energy (10.8 kJ mol^{-1}) is noted for the ring closing reaction (AA-NT1$_O$). For the other transition states, the solvation has no significant influence on the free energy profile.

Table 3. Standard Gibbs Free Energy for the Formation of the Prereaction Complex, $\Delta G°(COM_O)$ and for the Indirect Hydrogen Abstraction Reaction (A_O), $\Delta_r G°$, As Well As the Activation Gibbs Free Energy of the Indirect Hydrogen Abstraction Reaction, $\Delta^{\ddagger} G°$ (in kJ mol^{-1})[a]

systems		monoallylic	bisallylic
1,4-pentadiene + ·OH	$\Delta G°(COM_O)$	-	19.2
A	$\Delta_r G°(A_O)$	-	−169.5
this work	$\Delta^{\ddagger} G°(A_O)$	-	9.3
(2*Z*,5*Z*)-heptadiene + ·OH	$\Delta G°(COM_O)$	17.9	18.4
B	$\Delta_r G°(A_O)$	−134.2	−182.2
ref 17	$\Delta^{\ddagger} G°(A_O)$	29.3	5.7
(3*Z*,6*Z*)-nonadiene + ·OH	$\Delta G°(COM_O)$	24.3	21.3
C	$\Delta_r G°(A_O)$	−152.7	−169.0
ref 26	$\Delta^{\ddagger} G°(A_O)$	30.5	17.6
arachidonic acid + ·OH	$\Delta G°(COM_O)$	-	21.4
D	$\Delta_r G°(A_O)$	-	−175.9
this work	$\Delta^{\ddagger} G°(A_O)$	-	13.9

[a] A: QCISD(T)/cc-pVTZ//BH&HLYP/6-31G(d) level of theory. B: G3MP2//BH&HLYP/6-31G(d) level of theory. C: MPWB1K/MG3S//MPWB1K/6-31+G(d,p) level of theory. D: ONIOM(QCISD(T)/cc-pVTZ:BH&HLYP/6-31G(d))//BH&HLYP/6-31G(d) level of theory.

Initial steps of lipid peroxidation have been well studied with density functional methodology, both in the nonenzymatic process[26] as well as in the iron center of the (soybean) lipoxygenase enzyme.[27,28] Besides hydrogen abstraction, the addition of molecular oxygen is also included in the nonenzymatic study. These results, together with our previously published ones, are collected in Table 3. As one can see from this table, the Gibbs free energy of complex formation is in the range of 18.4 to 21.4 kJ mol^{-1}, depending on the methods used and the system studied; this difference is around the chemical accuracy. In contrast to this, the difference in the reaction Gibbs free energy of the bisallylic radical formation is about −169.0 kJ mol^{-1} for the 1,4-pentadiene + ·OH and (3Z,6Z)-nonadiene + ·OH reactions. The latter system was calculated at the MPWB1K//MG3S//MPWB1K/6−31+G(d,p) level of theory, and it was used by Tejero et al.[26] as a model for the lipid peroxidation of AA. The reaction Gibbs free energy of (2Z,5Z)-heptadiene + ·OH (calculated at the G3MP2//BH&HLYP/6−31G(d) level of theory) and AA + ·OH are also almost identical. The difference between the two groups is only 13 kJ mol^{-1}, which can be explained by the sum of several errors such as the difference in the computation methods. Surprisingly, the energetics of monoallylic and bisallylic hydrogen abstractions differ only by 16.3 kJ mol^{-1} in the case of the (3Z,6Z)-nonadiene + ·OH reaction system. That difference is 48 kJ mol^{-1} in the case of the (2Z,5Z)-heptadiene + ·OH reaction calculated at the G3MP2//BH&HLYP/6−31G(d) level of theory.[17]

Borowski et al.[27] published their theoretical work on the enzymatic process including the abstraction reaction and the O_2 addition. They studied the reaction between (Z,Z)-hepta-2,5-diene and the active site of the soybean enzyme (SLO-1). The initial structure of the active site is characterized by X-ray measurements. In this case, geometries were characterized using the B3LYP density functional and the LanL2DZ basis set with an effective core potential (ECP) for the Fe atom and the D95 basis set for H, C, N, and O atoms. The B3LYP/6−311+G(d,p) level of theory was used for single point calculations. The first catalytic step consisted of a hydrogen atom transfer from the hydrocarbon to the hydroxide group bound to the ferric ion. This process proceeds *via* an early transition state with the activation energy amounting to 50.6 kJ mol^{-1}, and the reaction energy is found to be −52.7 kJ mol^{-1}. This activation barrier seems to be quite high compared to our results of nonenzymatic hydrogen abstraction (with pseudo negative activation barrier). On the one hand, this result might be due to the inaccuracy of the available computational level for iron containing species. On the other hand, increased activation barrier in the enzymatic process can be the price paid for site-selective oxidation.

Tejero et al. also studied the (Z,Z)-hepta-2,5-diene + ·OH reaction[28] using a similar model for the enzymatic surroundings to that used by Borowski. They reported that the standard Gibbs free energy barrier for the hydrogen abstraction was as high as 87.0 kJ mol^{-1}, obtained using the B3LYP/6−311+G(d,p)//B3LYP/LanL2DZ level of theory. However, the differences between Borowski's and Tejero's results might arise mainly from conformational differences or because the extended model involving iron could be calculated only at lower accuracy.

The evolution of living organisms in an oxidizing atmosphere has resulted in a complex array of antioxidation mechanisms within cells to protect critical biomolecules from oxidative modifications. Because lipids are often the initial barrier to the free diffusion of reactive oxygen species into the cell, they themselves become targets of nonenzymatic oxidation reactions.[29] These nonenzymatic processes result in a wide variety of products having diverse biological functions, such aldehydes, shorter fatty acids, and isoprostanoids. While the first two groups are toxic, isoprostanoids with appropriate chirality (and within a certain concentration range) are essential for living cells. In addition, our calculations suggest that nonenzymatic formation of isoprostanoids is energetically favored. Based on these facts, we might suspect that in the course of biomolecular evolution, these nonenzymatic processes predated the enzymatic ones. Specific enzymes might have evolved for the purpose of controlling selectivity (the required products and their appropriate stereochemistry).

4. Conclusion

Employing the 1,4-pentadiene + ·OH reaction system, the energetically preferred oxidation pathways are studied for the PUFA using first-principles methods. We find that the terminal and nonterminal additions and the indirect hydrogen abstraction reaction have pseudonegative activation enthalpies due to the prereaction complex. The H-abstraction is found to be the most exothermic reaction among those studied (−167.9 kJ mol^{-1}).

The nonterminal adduct (the 4-pentene-2-ol-1-yl radical) is able to react forward to produce cyclopentanol-3-yl radical as product. The enthalpy level of the cyclopentanol-3-yl radical is 26.4 kJ mol^{-1} lower than that of the product of the hydrogen abstraction. The activation enthalpy of this ring closing reaction is significantly smaller than the exothermicity of the nonterminal addition. Consequently, this reaction is expected to be fast. Furthermore, there is also a possible channel for bond scission,

which gives allyl radical and vinyl alcohol as products. Although this reaction is slightly endothermic, its activation enthalpy is still below the entrance enthalpy level of the 1,4-pentadiene + •OH reaction by 25.5 kJ mol^{-1}.

Since the PUFA have very often a −HC=CH−CH_2−CH=CH− moiety, one of them, arachidonic acid (AA), is studied as an analog to the reaction between 1,4-pentadiene and the hydroxyl radical. The thermodynamic properties obtained using the ONIOM technique for AA and QCISD(T)/cc-pVTZ//BH&HLYP/6−31G(d) for 1,4-pentadiene are found to be similar. Nonenzymatic ring closing and bond scission can also be energetically favored since the energetics of the transition states are still below the entrance enthalpy level (AA + •OH). As far as we know, our results demonstrate for the first time a possible, *ab initio*-based mechanism for the nonenzymatic biosynthesis of isoprostane-like structures from AA without the presence of molecular oxygen.

It is believed that the nonenzymatic ring closing and bond scission can also occur in the case of other PUFAs, such as docosahexaenoic acid (DHA).

Although these nonenzymatic radical reactions are energetically favored and they can occur in biological systems as spontaneous and fast processes, they are not selective. Specific enzymes might be responsible mainly for controlling the required products and their appropriate stereochemistry.

Acknowledgment. The authors thank Máté Labádi for excellent technical support. The authors are also grateful to Steven Neshyba and Claudio Morgado for their excellent suggestions.

Supporting Information Available: Reaction scheme for all possible indirect reactions of 1,4-pentadiene and •OH (indicated values are relative energies with zero-point correction related to the level of 1,4-pentadiene + •OH obtained by the BH&HLYP/6−31G(d) level of theory). This material is available free of charge via the Internet at http://pubs.acs.org.

References

(1) Sprecher, H. *Prog. Lipid Res.* **1986**, *25*, 19.

(2) Morrow, J. D.; Awad, J. A.; Wu, A.; Zackert, W. E.; Daniel, V. C.; Roberts, L. J. *J. Biol. Chem.* **1996**, *271*, 23185.

(3) Wainwright, P. E. *Neurosci. Biobehav. Rev.* **1992**, *16*, 193.

(4) Voet, D.; Voet J. *Biochemistry*; John Wiley & Sons Inc.: New York, NY, 1990; p 658.

(5) McMurry, J. E.; Begley, T. P. *The Organic Chemistry of Biological Pathways*; Roberts and Company Publisher: Englewood, CO, 2005; pp 364−368.

(6) Davis, T. A.; Gao, L.; Yin, H.; Morrow, J. D.; Porter, N. A. *J. Am. Chem. Soc.* **2006**, *128*, 14897.

(7) Yin, H.; Gao, L.; Tai, H. H.; Murphey, L. J.; Porter, N. A.; Morrow, J. D. *J. Biol. Chem.* **2007**, *282*, 329.

(8) Yoshino, K.; Sano, M.; Fujita, M.; Tomita, I. *Chem. Pharm. Bull.* **1991**, *39*, 1788.

(9) Frisch, M. J.; Trucks, G. W.; Schlegel, H. B.; Scuseria, G. E.; Robb, M. A.; Cheeseman, J. R.; Montgomery, J. A., Jr.; Vreven, T.; Kudin, K. N. ; Burant, J. C.; Millam, J. M.; Iyengar, S. S.; Tomasi, J.; Barone, V.; Mennucci, B.; Cossi, M.; Scalmani, G.; Rega, N.; Petersson, G. A.; Nakatsuji, H.; Hada, M.; Ehara, M.; Toyota, K.; Fukuda, R.; Hasegawa, J.; Ishida, M.; Nakajima, T.; Honda, Y. ; Kitao, O.; Nakai, H.; Klene, M.; Li, X.; Knox, J. E.; Hratchian, H. P.; Cross, J. B.; Bakken, V.; Adamo, C.; Jaramillo, J.; Gomperts, R.; Stratmann, R. E.; Yazyev, O. ; Austin, A. J. ; Cammi, R.; Pomelli, C.; Ochterski, J. W.; Ayala, P. Y.; Morokuma, K.; Voth, G. A.; Salvador, P.; Dannenberg, J. J.; Zakrzewski, V. G.; Dapprich, S.; Daniels, A. D.; Strain, M. C.; Farkas, O.; Malick, D. K.; Rabuck, A. D.; Raghavachari, K.; Foresman, J. B.; Ortiz, J. V.; Cui, Q.; Baboul, A. G.; Clifford, S.; Cioslowski, J.; Stefanov, B. B.; Liu, G.; Liashenko, A.; Piskorz, P.; Komaromi, I.; Martin, R. L.; Fox, D. J.; Keith, T.; Al-Laham, M. A.; Peng, C. Y.; Nanayakkara, A.; Challacombe, M.; Gill, P. M. W.; Johnson, B.; Chen, W.; Wong, M. W.; Gonzalez, C.; Pople, J. A. *GAUSSIAN03, (Revision C.02)*; Gaussian, Inc.: Wallingford, CT, 2004.

(10) Szori, M.; Fittschen, C.; Csizmadia, I. G.; Viskolcz, B. *J. Chem. Theory Comput.* **2006**, *2*, 1575.

(11) Purvis, G. D.; Bartlett, R. J. *J. Chem. Phys.* **1982**, *76*, 1910.

(12) Gauss, J.; Cremer, D. *Chem. Phys. Lett.* **1988**, *150*, 280.

(13) Salter, E. A.; Trucks, G. W.; Bartlett, R. J. *J. Chem. Phys.* **1989**, *90*, 1752.

(14) Kendall, R. A., Jr.; Harrison, R. J. *J. Chem. Phys.* **1992**, *96*, 6796.

(15) Dapprich, S.; Komaromi, I.; Byun, K. S.; Morokuma, K.; Frisch, M. J. *J. Mol. Struct. (THEOCHEM)* **1999**, *461*, 1.

(16) Barone, V.; Cossi, M. *J. Phys. Chem. A* **1998**, *102*, 1995.

(17) Szori, M.; Abou-Abdo, T.; Fittschen, C.; Csizmadia, I. G.; Viskolcz, B. *Phys. Chem. Chem. Phys.* **2007**, *9*, 1931.

(18) Sosa, C.; Schlegel, H. B. *J. Am. Chem. Soc.* **1987**, *109*, 4193.

(19) Szori, M.; Viskolcz, B. *J. Mol. Struct. (THEOCHEM)* **2003**, *666*, 153.

(20) Battin-Leclerc, F. *Phys. Chem. Chem. Phys.* **2002**, *4*, 2072.

(21) Skjoth-Rasmussen, M. S.; Glarborg, P.; Ostberg, M.; Johannessen, J. T.; Livbjerg, H.; Jensen, A. D.; Christensen, T. S. *Combust. Flame* **2004**, *136*, 91.

(22) Zielinska, B.; Sagebiel, J. C.; Harshfield, G.; Gertler, A. W.; Pierson, W. R. *Atmos. Environ.* **1996**, *30*, 2269.

(23) Reducing Emissions. 2005. Canadian Chemical Producers' Association Web Site. http://www.ccpa.ca/files/Library/Reports/NERM14_2005/RE14_Report07EN.pdf (accessed June, 4, 2008).

(24) Law, J. M. S.; Szori, M.; Izsak, R.; Penke, B.; Csizmadia, I. G.; Viskolcz, B. *J. Phys. Chem. A* **2006**, *110*, 6100.

(25) Kitaguchi, H.; Ohkubo, K.; Ogo, S.; Fukuzumi, S. *Chem. Commun.* **2006**, *9*, 979.

(26) Tejero, I.; González-Lafont, A.; Lluch, J. M.; Eriksson, L. A. *J. Phys. Chem. B* **2007**, *111*, 5684.

(27) Borowski, T.; Broćławik, E. *J. Phys. Chem. B,* **2003**, *107*, 4639.

(28) Tejero, I.; Eriksson, L. A.; González-Lafont, A.; Marquet, J.; Lluch, J. M. *J. Phys. Chem. B* **2004**, *108*, 13831.

(29) Smith, W. L.; Murphy, R. C. *J. Bio. Chem.* **2008**, *283*, 15513.

CT800127A